



A multidating approach applied to historical slackwater flood deposits of the Gardon River, SE France

L. Dezileau, B. Terrier, J.F. Berger, P. Blanchemanche, A. Latapie, R. Freydier, L. Bremond, André Paquier, M. Lang, J.L. Delgado

► To cite this version:

L. Dezileau, B. Terrier, J.F. Berger, P. Blanchemanche, A. Latapie, et al.. A multidating approach applied to historical slackwater flood deposits of the Gardon River, SE France. *Geomorphology*, 2014, 214, p. 56 - p. 68. 10.1016/j.geomorph.2014.03.017 . hal-01059669

HAL Id: hal-01059669

<https://hal.science/hal-01059669>

Submitted on 1 Sep 2014

HAL is a multi-disciplinary open access archive for the deposit and dissemination of scientific research documents, whether they are published or not. The documents may come from teaching and research institutions in France or abroad, or from public or private research centers.

L'archive ouverte pluridisciplinaire **HAL**, est destinée au dépôt et à la diffusion de documents scientifiques de niveau recherche, publiés ou non, émanant des établissements d'enseignement et de recherche français ou étrangers, des laboratoires publics ou privés.

A multidating approach applied to historical slackwater flood deposits of the Gardon River, SE France

L.Dezileau^{a,*}, B.Terrier^b, J. F.Berger^c, P.Blanchemanche^d, A.Latapie^e,
R.Freydier^f, L.Bremond^g, A.Paquier^e, M.Lang^e, J.L.Delgado^h

^aGeosciences Montpellier, Université Montpellier 2, CNRS, UMR 5243, France

^bAgence de l'eau Rhône-Méditerranée et Corse, Lyon cedex, France

^cEnvironnement Ville et Société, Université Lumière Lyon 2, CNRS, France

^dArchéologie des Sociétés Méditerranéennes, CNRS, UMR 5140, France

^eIrstea, UR HHLY, CS 70077, Villeurbanne, France

^fHydrosciences Montpellier, Université Montpellier 2, CNRS, UMR 5569, France

^gCentre de Bio-Archéologie et d'Ecologie, EPHE, Université Montpellier 2, CNRS, UMR 5059, France

^hCETE Méditerranée, Aix-en-Provence, France

* Corresponding author: UMR 5243 CC60 UM2/CNRS, Place E. Bataillon 34095 Montpellier cedex 5, France. Fax:
+33 (0) 4 67 14 49 30 ;E-mail: laurent.dezileau@gm.univ-montp2.fr.

Geomorphology, 214, 56-68, <http://dx.doi.org/10.1016/j.geomorph.2014.03.017>

Abstract

A multidating approach was carried out on slackwater flood deposits, preserved in valley side rock cave and terrace, of the Gardon River in Languedoc, southeast France. Lead-210, caesium-137, and geochemical analysis of mining-contaminated slackwater flood sediments have been used to reconstruct the history of these flood deposits. These age controls were combined with the continuous record of Gardon flow since 1890, and the combined records were then used to assign ages to slackwater deposits. The stratigraphic records of terrace GE and cave GG were excellent examples to illustrate the effects of erosion/preservation in a context of a progressively self-censoring, vertically accreting sequence. The sedimentary flood record of the terrace GE located at 10 m above the channel bed is complete for years post-1958 but incomplete before. During the 78-year period 1880-1958, 25 floods of a sufficient magnitude ($> 1450 \text{ m}^3/\text{s}$) have covered the terrace. Since 1958, however, the frequency of inundation of the deposits has been lower: only 5 or 6 floods in 52 years have been large enough to exceed the necessary threshold discharge ($> 1700 \text{ m}^3/\text{s}$). The progressive increase of threshold discharge and the reduced frequency of inundation at the terrace could allow stabilisation of the vegetation cover and improved protection against erosion from subsequent large magnitude flood events. The sedimentary flood record seems complete for cave GG located at 15 m above the channel bed. Here, the low frequency of events would have enabled a high degree of stabilisation of the sedimentary flood record, rendering the deposits less susceptible to erosion. Radiocarbon dating are used in this study and compared to the other dating techniques. Eighty percent of radiocarbon dates on charcoals were considerably older than those obtained by the other techniques in the terrace. On the other hand, radiocarbon dating on seeds provided better results. This discrepancy between radiocarbon dates on charcoal and seeds is explained by the

nature of the dated material (permanent wood vs. annual production and resistance to degradation process). Finally, we showed in this study that although the most common dating technique used in paleoflood hydrology is radiocarbon dating, usually on charcoal preserved within slackwater flood sediments, this method did not permit us to define a coherent age model. Only the combined use of lead-210, caesium-137, and geochemical analysis of mining-contaminated sediments with the instrumental flood record can be applied to discriminate and date the recent slackwater deposits of the terrace GE and cave GG.

Keywords: paleoflood hydrology; floods; hydraulic modelling; lead-210; caesium-137; radiocarbon dating; historical record of mining activity

1. Introduction

Palaeoflood hydrology is the reconstruction of the magnitude and frequency of large floods using geological evidence (Baker et al., 2002). Methods and concepts of paleohydrology have been described extensively in the literature (e.g., Kochel et al., 1982; Ely and Baker, 1985; Baker, 1987; Benito and Thorndycraft, 2005). Only some of the general concepts are briefly reiterated here. The methodology combines (i) stratigraphic and sedimentologic analyses to identify the number of flood units preserved within a particular sedimentary sequence; (ii) hydraulic modelling to calculate minimum discharge estimates from the known elevations of slackwater flood sediments; (iii) dating techniques to determine the chronology of flood occurrence; and (iv) establishment of possible links between past climatic changes and the frequency/magnitude of flood events. Although the main aim of palaeoflood hydrology is to lengthen the flood series beyond that of the instrumental record, significant benefits can also be gained by accurately dating modern slackwater flood deposits (Thorndycraft et al., 2004a,b). As these events occurred

during the instrumental period, the potential to correlate the modern sedimentary flood record with the data measured at gauging stations is possible. This is of particular importance in understanding the palaeoflood record preserved over centennial timescales (Benito et al., 2004).

In this study, ^{14}C , ^{210}Pb , and ^{137}Cs dating and geochemical analyses (Pb and Al concentrations) were carried out on slackwater flood deposits, preserved in valley side rock cave and terrace, of the Gardon River in Languedoc in southeast France (Fig. 1). The study sites are located near Remoulins where a gauging station has been operational over the last 130 years. This provided the potential for correlation between the instrumental and sedimentary flood records. The two largest floods of the twentieth and twenty-first centuries, namely the 1958 and 2002 events (with estimated discharges of $6400 \text{ m}^3/\text{s}$ and $7200 \text{ m}^3/\text{s}$, respectively, at Remoulins, compared to a mean annual flow of $33 \text{ m}^3/\text{s}$) occurred during the dating range of the ^{137}Cs and ^{210}Pb methods, thereby providing the potential for comparison between these events and palaeofloods. Finally, our analysis of slackwater flood deposits illustrates important uncertainties related to stratigraphic studies of paleofloods. These uncertainties bear directly on related limitations in individual event discrimination and temporal resolution of typical slackwater paleoflood records caused by effects of erosion/preservation in a context of a progressively self-censoring vertically accreting sequence.

2. Dating techniques

Different techniques are available to date recent slackwater deposits. ^{137}Cs dating has been used for determining the chronology of modern sediment deposits. ^{137}Cs is an artificial radionuclide that was first released into the atmosphere by nuclear bomb testing in the mid-1950s. The

temporal patterns of ^{137}Cs input are characterized by a first peak in 1959 and a second peak at 1962-1964; the termination of ^{137}Cs input occurred around mid-1980s. Some areas may have had an additional input in 1986 after the Chernobyl incident. ^{137}Cs reached the land surface by atmospheric fallout. The accumulation of ^{137}Cs in sedimentary deposits throughout the world therefore began by the early to mid-1950s (e.g., Popp et al., 1988). Analysis of ^{137}Cs has been applied to fine-grained deposits to quantify soil erosion and lake sedimentation rates (e.g., Ritchie et al., 1974; Sutherland, 1989), to date oxbow sedimentation and modern fine-grained floodplain sediments (Popp et al., 1988; Walling and He, 1997; Bonté et al., 2001; Stokes and Walling, 2003). However, ^{137}Cs is strongly adsorbed to clay particles and is transported with the suspended load rather than in solution (McHenry and Ritchie, 1977). The detectable activity of ^{137}Cs is related to the clay content of the sediments (McHenry and Ritchie, 1977; Popp et al., 1988), which poses a potential problem when the technique is applied to alluvial deposits with relatively low clay content. Studies analysing the post-bomb ^{137}Cs content in modern slackwater flood deposits from the San Francisco, Paria rivers in Arizona and from the Llobregat River in Spain (Ely et al., 1992; Thorndycraft et al., 2005b) have shown that the technique can also be successfully applied to date fluvial sediments characterized by a mix of fine and coarser particles. The ^{137}Cs dating results from the Gardon River study reaches can be tested using the combined data of palaeoflood stratigraphy, discharge estimation by hydraulic modelling and the instrumental discharge record.

The basic methodology of ^{210}Pb dating was established in a seminal paper by Golberg (1963). ^{210}Pb precipitates from the atmosphere through ^{222}Rn decay and accumulates in surface soils, glaciers, or lakes where successive layers of material are buried by later deposits. ^{210}Pb deposition on land is primarily owing to meteoric fallout; and it is adsorbed quickly and

tenaciously by the surfaces of fine sediments, primarily onto clays, where, even more so than ^{137}Cs , it is chemically immobile (Cremers et al., 1988). There it undergoes beta decay to ^{210}Bi with a half-life of 22.3 years. ^{210}Pb fallout is generally found to be constant at any given location over time scales relevant to ^{210}Pb geochronology (Appleby and Oldfield, 1978, 1992; He and Walling, 1996). In the simplest model, the initial $(^{210}\text{Pb})_{\text{ex}}$ is assumed constant and thus $(^{210}\text{Pb})_{\text{ex}}$ at any time is given by the radioactive decay law. The sedimentation rates in slackwater flood deposits are clearly variable and discontinuous because of the near-instantaneous sedimentation of flood deposits so that this type of model is difficult to use (He and Walling, 1996; Aalto and Nitttrouer, 2012). However, this technique can be successfully applied to assess whether an apparent accumulation of 'fresh sediment' exists (<100 years, i.e., ~4 to 5 times its decay period of 22.3 years). ^{210}Pb dating will be tested in the Gardon River.

Carbon-14 analysis is the standard technique for dating Holocene alluvial deposits. Radiocarbon dating of slackwater flood sediments has an applicable age range of between ca. 300 and 55,000 yBP (Trumbore, 2000) and therefore cannot accurately date the sediments of flood events from the most recent centuries. With atmospheric testing of nuclear weapons after 1950, ^{14}C activity in the troposphere rapidly increased, reaching a peak of 100% above normal in the early 1960s (Nydal and Lovseth, 1983). For post-bomb alluvial deposits, radiocarbon dating on organic materials preserved within slackwater flood sediments gives a 'modern age' that can be useful to assess whether an apparent accumulation of "fresh sediment" exists in the study area. The ^{14}C age of organic materials entrained in an alluvial deposit may differ significantly from the actual age of the deposit, depending on the residence time of the organics within the environment (Ely et al., 1992). Thus, for flood deposits, the type of organic material available constrains the accuracy of the resulting dates. In particular, detrital wood and charcoal can predate fluvial deposits by

several hundred years (Atwater et al., 1990). The radiocarbon dating is not the best technique to accurately date the sediments of flood events from the most recent centuries (Trumbore, 2000) but was used in this study to be tested by obtaining radiocarbon dates for several types of plant materials from well-dated flood deposits.

Ages for modern flood deposits can be correctly assigned with the use of trace metals generated by mining activity. This geochemical analysis of mining-contaminated floodplain sediments has been used to date floodplain sediment and slackwater flood deposits where a known historical record of mining within the catchment exists (e.g., Davies and Lewin, 1974; Lewin et al., 1977; Hindel et al., 1996; Knox and Daniels, 2002; Thorndycraft et al., 2004a,b). The extraction of Zn–Pb from the Gardon River basin started in 1730 (Elbaz-Poulichet et al., 2006). The number of mining concessions increased significantly between 1860 and 1930. During this period, mining activity generated 400,000 tons of tailings. Between 1951 and 1963, Pennaroya and then Metaleurop mining companies extensively exploited the ore generating between 2,300,000 and 5,000,000 tons of tailings (30,000 tons of lead and 3500 tons of Zn). This mining activity ceased in 1993. One of the most important mines on the Gardon River basin is the Carnoules mine, which has generated a total of 1,500,000 tons of wastes. The mine officially closed on 24 October 1963. In September 1976, the tailings partially collapsed caused by a violent Mediterranean thunderstorm. This was followed in October 1976 by the sudden evacuation of the 100,000 m³ of water initially contained in a lake that had formed in the tailing stock. The accident was responsible for a major pollution of water and soil in the Gardon River basin (DREAL, 2008). This paper describes a combined stratigraphic and geochemical approach to identify traces of historic tin mining activity within slackwater deposits of the Gardon River.

3. Gardon River basin flood hydrology

3.1. Study area description

The Gardon River watershed (1858 km² at Remoulins) is located in the southeast Massif Central mountains and is ~ 135 km long from its headwaters at 1699 m above sea level (Mount Lozère) to its confluence with the Rhône River at 6 m asl (Fig. 1A). The Gardon is the southern most tributary of the Rhône River. In terms of geology (Fig. 1B), the Cévennes Mountains are mainly composed of Paleozoic granite, schist, gneiss, and sandstone (Bonnifant et al., 2009). The rivers present a high degree of sinuosity in this upstream area. Farther downstream, the Gardon River crosses the Gard plains, which are based on Mesozoic carbonate formations with a stratigraphical series ranging from Jurassic (west) to Cretaceous (east). Close to the Cévennes Mountains, this secondary series is interrupted by a network of NE–SW faults that delineate the Alès graben, a 1500-m graben filled with Tertiary sediments from the Oligocene period. The river then crosses Cretaceous limestone following deep canyons (the Gardon gorges). These limestone formations present a high degree of karstification. Downstream, the Mesozoic formations are covered with the Quaternary sediments of the Rhône River (Bonnifant et al., 2009). The high watershed of the Gardon River was reforested during the nineteenth century by calcic or acidophile medio-European beech species, white oak species, *Castanea sativa* forests, and shrublands with *Juniperus communis*. The limestone tableland of Nîmes garrigue, mainly occupied by forests of green oaks (*Quercus ilex* and *Quercus rotundifolia*), some white oak coppice, a mosaic of a substeppic grassland with annual grasses from the *Thero-brachypodietea*. The Matorral tree with *Juniperus phoenicea* occupies the rocky ledges of the limestone tableland, while on the rocky slopes develop xero-thermophilic formations with *Buxus sempervirens*. The limestone canyon includes riparian vegetation composed mainly of *Salix alba*, *Populus alba*, and *Fraxinus*

excelsior, with some pines (*Aleppo* and *Pinion pines*) on pediments and upper alluvial terraces.

Insert Fig. 1 near here

The study sites are located in the middle reach of the Gardon River in the Cretaceous bedrock gorge, between Russan and Remoulins. Little to no changes in the shape of the canyon occurred throughout the late Holocene. The identification of flood sediment sources transported into the gorge is facilitated by the strong contrast between the granitic, basaltic, and metamorphic bedrock of the upper catchment and the carbonates of the Gardon gorge. Slackwater flood sediments have been deposited and preserved on high-standing terraces along channel margins and in many karstic caves and alcoves.

3.2. Flood hydrology and hydroclimatology

The Gardon River has a typically Mediterranean regime with a low mean annual discharge (33 m³/s, SAGE des Gardons, 2000), extreme seasonal variations, and flood peaks around 100 times greater than the mean discharge. Mean annual rainfall in the catchment varies from 500 to 1100 mm. Nuissier et al. (2008) provided a detailed analysis of typical flash flood events in this region. Large amounts of precipitation can accumulate over several days, particularly at the end of summer and beginning of autumn, as frontal disturbances slow down and are reinforced by the relief of the Massif Central. When a Mesoscale Convective System remains quasistationary for several hours, heavy rainfall of over 200 mm can be recorded in less than a day and can therefore lead to devastating flash floods.

A large set of hydrological data is available from the flood forecasting service (known as the ‘Service de Prevision des Crues’ or SPC30) and the local authority (‘Smage des Gardons’). The gauging station located at Remoulins (~15 km downstream of study sites) provides stage observations from 1890 onward (Fig.2). Since 1890, three major flood events have been recorded with water levels > 7 m and estimated peak flood discharges defined from the stage-discharge relationship > 5000 m³/s, namely the 16-17 October 1907 (5300 m³/s), 4 October 1958 (6400 m³/s), and 8-9 September 2002 (7000 m³/s) floods. This last extreme flood event claimed the lives of 23 people and caused €1.2 billion worth of damage to towns and villages along the river. Seven thousand houses were damaged, 100 of which were completely destroyed and 1500 submerged under 2 m of water (Huet et al., 2003).

Insert Fig. 2 near here

3.3. Previous paleoflood studies of the Gardon River

One paleoflood study of the Gardon River has been conducted just downstream of our study area (Sheffer et al., 2008). The main objectives of their study were (i) to provide an accurate and reliable discharge estimation of the 2002 flood at the study reach, (ii) to reconstruct a record of major flood events using paleoflood hydrology, and (iii) to improve the understanding of the 2002 flood magnitude and consider the long-term perspective of rare events and extreme flood discharges provided by the paleoflood record. They concluded that according to slackwater deposits found at different sites at least five extreme events occurred during the Little Ice Age. Each was larger than the 2002 flood (Sheffer et al., 2008).

4. Methods

4.1. Paleoflood analysis

During large floods in canyons, slackwater deposits(usually fine sands and silts) accumulate relatively rapidly from suspension in sites of abrupt drop in flow velocity (Ely and Baker, 1985; Kochel and Baker, 1988; Benito et al., 2003a). As a result, a layer of these deposits is formed. This sediment may be preserved in protected sites, such as caves and alcoves in the canyon walls, and backwater zones behind valley constrictions (Kochel et al., 1982; Ely and Baker, 1985; Baker and Kochel, 1988; Enzel et al., 1994; Springer, 2002; Webb and Jarrett, 2002; Benito et al., 2003b; Benito and Thorndycraft, 2005). Subsequent flood deposits may accumulate above this layer by floods with stages higher than the top of the depositional sequence (Baker, 1987).

For this study, two depositional sequences (Fig. 3) were investigated along the Gardon River in a high-standing, terrace-like bench of aggrading sediments (GE located at 10 m above the channel bed, the base of the terrace is at 2 m, the terrace is 70 m wide and 300 m long) and in a cave (GG at 15 m above the channel bed). Sites of slackwater flood sediment deposition were identified along the study reaches, and sections were cut to expose the sedimentary sequences. Individual flood units were determined through a close inspection of depositional breaks and/or indicators of surficial exposure (e.g., presence of a paleosol, clay layers at the top of a unit, detection of erosional surfaces, bioturbation features, angular clast layers deposits in local alcoves or slope material accumulation between flood events, fireplaces, and anthropogenic occupation layers between flood events).

Insert Fig. 3 near here

4.2. Analytical methods

Dating of sedimentary layers was carried out using ^{210}Pb and ^{137}Cs methods on a centennial timescale. Both nuclides together with U, Th, and ^{226}Ra were determined by gamma spectrometry at the Géosciences Montpellier Laboratory. The 1-cm-thick sediment layers were sieved in order to obtain the fraction smaller than 1 mm. This material was then finely crushed after drying and transferred into small gas-tight PETP (polyethylene terephthalate) tubes (internal height and diameter of 38 and 14 mm, respectively), and stored for more than 3 weeks to ensure equilibrium between ^{226}Ra and ^{222}Rn . The activities of the nuclides of interest were determined using a Canberra Ge well detector and compared with the known activities of an in-house standard. Activities of ^{210}Pb were determined by integrating the area of the 46.5-keV photo-peak. ^{226}Ra activities were determined from the average of values derived from the 186.2-keV peak of ^{226}Ra and the peaks of its progeny in secular equilibrium with ^{214}Pb (295 and 352 keV) and ^{214}Bi (609 keV). In each sample, the (^{210}Pb unsupported) excess activities were calculated by subtracting the (^{226}Ra supported) activity from the total (^{210}Pb) activity. Note that, throughout this paper, parentheses () denote activities. Activities of ^{137}Cs were determined by integrating the area of the 661-keV photo-peak. Error bars on ($^{210}\text{Pbex}$) and (^{137}Cs) do not exceed 6%.

The ^{14}C analyses were conducted at the Laboratoire de Mesure ^{14}C (LMC14) on the ARTEMIS accelerator mass spectrometer in the CEA Institute at Saclay (Atomic Energy Commission). These ^{14}C analyses were carried out with the standard procedures described by Tisnérat-Laborde et al. (2001). The ^{14}C ages were converted to calendar years using the CALIB 6.1.0 calibration program (Stuiver and Reimer, 1993). A summary of the samples submitted for dating, and their associated results, is presented in Table 1. All radiocarbon dates are quoted in the text as the 2σ calibrated age range.

284

285

Insert Table 1 near here

286

287

288 Before analysis, sediment samples were ground in an agate mortar and digested in a Teflon beaker
289 on a hot plate. One hundred milligrams of sediment were digested using a three step procedure:
290 1/H₂O₂, 2/HF:HNO₃:HClO₄, and 3/HNO₃:HCl. The Al and Pb concentrations were determined
291 using an ICP-MS, X Series II (Thermo Fisher Scientific), equipped with a CCT (Collision Cell
292 Technology) chamber at the Hydrosiences Montpellier Laboratory. Certified reference material
293 from LGC Standards, i.e., LGC6189 (river sediment), was used to check analytical accuracy and
294 precision. Measured concentrations agree with recommended values to within 10% (Al) and 3%
295 (Pb). To find out if there was an enrichment of lead relative to the local baseline, an enrichment
296 factor (EF) technique was used. The enrichment factor (EF) of lead is calculated following the
297 equation: $EF_{Pb} = (Pb/Al)_{sample} / (Pb/Al)_{Average\ Local\ Background}$.

298 The $(Pb/Fe)_{sample}$ is the ratio of Pb and Fe concentration of the sample and $(Pb/Fe)_{Average\ Local}$
299 $background$ is the ratio of Pb and Fe concentration of a background. The background concentrations
300 of Pb were taken from the base of the terrace (i.e., pre-industrial period concentrations).
301 Grainsize analysis was conducted on contiguous 1 cm samples using a Beckman-Coulter
302 LS13320 laser diffraction particlesize analyser at the Géosciences Montpellier Laboratory. Grain
303 size distribution measurements were made on the < 1 mm sediment fraction.

304

305 *4.3. Hydraulic modelling*

306 *4.3.1. Model description*

A one-dimensional (1D) hydraulic model of the Gorges was built using RubarBE, a numerical model that solves the shallow water equations and uses an explicit second-order Godunov-type scheme (El kadi Abderrezzak and Paquier, 2009). The modelled reach is ~31.5 km long and extends from Russan, located at the entrance of the Gorges, to downstream of the Remoulins gauging station, located at the exit of the Gorges. Topographic data were obtained from the SPC30 and the Smage des Gardons. In addition, two surveying campaigns were carried out in the Gorges in order to obtain detailed topographic data near the paleoflood sites. During these campaigns, 21 profiles were surveyed with a Leica TC 305 total station and a differential GPS Leica 1200 with GPS-GLONASS receptor. In total, 95 profiles were used to construct the hydraulic model. The 2002 flood hydrographs provided by the SPC30 at Russan and Remoulins gauging stations revealed that the peak flows were approximately the same at both locations. In order to simulate past flood events, it was therefore decided that the flow at Remoulins be used as an upstream boundary condition at Russan. The downstream boundary condition has been defined with the water levels available at the Remoulins gauging station.

A sensitivity analysis has been conducted to assess the influence of the Alzon River, a tributary draining an area of 203 km², on the water levels calculated at the paleoflood sites.

4.3.2. Model calibration

Following the 2002 flood event, a post-event analysis of debris lines and observed water levels was conducted by the Smage des Gardons. The model was thus calibrated on the 21 water levels available for the 2002 event and validated on the 10 water levels recorded for the 1958 event. On average, the difference between the measured water levels and the results of the model is -0.11 m with a standard deviation of 0.69 m for the 2002 flood event. For the 1958 event, the average difference is -0.95 m with a standard deviation of 0.94 m. Most of the debris lines surveyed are

located in the vicinity of hydraulic singularities such as bridges. The flow behaviour in these areas is notably difficult to reproduce in a 1D hydraulic model. Furthermore, the levels of the debris lines in the vicinity of the bridge may not be representative of the highest mean water level and may be the result of water surface fluctuations that cannot be reproduced by the 1D model. The results of the calibration are therefore regarded as satisfactory.

Insert Fig. 4 near here

4.3.2. Sensitivity analysis

The results of the model with the varying roughness coefficient allow the determination of an envelope of stage discharge relationship at the two paleoflood sites (Fig. 4B). The sensitivity analysis on the flow record used as an upstream boundary condition in the model also provides an envelope on the water levels and discharges at the paleosites for each flood event. Results are then compared with the historical flood records available at Remoulins to identify the events that may have reached or submerged the sites (Fig. 4C). Envelopes at the paleoflood sites are bound by the scenarios of the sensitivity analysis of $Q \pm 10\%$ combined with the scenarios of $K_s \pm 10\%$. These results can be put into perspective with the dating approach and are discussed in the following paragraphs.

5. Results

5.1. Stratigraphic records of flood events in terrace GE and cave GG

5.1.1. Terrace GE

At terrace GE, the stratigraphy consists of 20 individual slackwater flood units. Based on the

results of the hydraulic model (stage-discharge curve), a flood event of intensity similar to that of the 1972 event ($\sim 2100 \text{ m}^3/\text{s}$ at Remoulins) is required for a flood event to cover the uppermost flood unit of the terrace. Figure 5 presents $^{210}\text{Pb}_{\text{ex}}$ and ^{137}Cs activities and the enrichment factor of Pb for this terrace. Also illustrated is the minimum discharge estimate calculated for the floodwaters to cover the terrace during flood events.

The ^{137}Cs activity is recorded in flood units GE17, GE18, GE19, and GE20, with maximum values of 38 and 45 mBq/g in units GE17 and GE18, respectively (Fig.5). No ^{137}Cs is found in the older deposits of the profile. The first post-1955 event, identified by the first trace of ^{137}Cs activity in the profile, is that of GE17 indicating that the four flood deposits GE17-GE20 all post-date this period. More particularly, the high ^{137}Cs activity recorded in flood units GE17 and GE18 (38 and 45 mBq/g) can be associated to the maximum atmospheric production in the mid-1960s (around 1963, Fig. 5).

The first flood unit containing $^{210}\text{Pb}_{\text{ex}}$ activity is unit GE15 located at 90 cm depth in the stratigraphic profile, with a value of 5 mBq/g. The $^{210}\text{Pb}_{\text{ex}}$ activity is recorded in flood units GE15, GE17, GE18, GE19, and GE20, with a maximum value of 58 mBq/g in unit GE19. There is an apparent accumulation of ‘fresh sediment’ (< 100 years, i.e., approximately 4 to 5 times the decay period of ^{210}Pb) in the uppermost part of the terrace GE. The $^{210}\text{Pb}_{\text{ex}}$ can help us to confirm a number of results produced using ^{137}Cs dating technique. The high $^{210}\text{Pb}_{\text{ex}}$ activity recorded in flood units GE19 and its exponential decrease in the other flood deposits (GE18 to G15) suggests that the uppermost part of the terrace can be considered as being stratifically undisturbed. In particular, the first trace of $^{210}\text{Pb}_{\text{ex}}$ activity in the profile is that of GE15, thereby indicating that the six flood deposits GE15-GE20 are recent and all post-date approximately the end-1910s (Fig. 7).

The geochemistry of the profile shows that enrichment factor (EF) of Pb, with a range of 1.0 to 10.5, exhibits very high variation between the base and the top of the terrace (Fig. 5). The lowest EF values of Pb (around 1.0) occur in flood units between GE1 and GE9. The EF is higher in the uppermost flood units of the terrace, around 1.9 between GE10 and GE17, 3.3 in GE18, 10.5 in GE19, while it decreases in the last flood unit GE20 (3). At 155 cm depth, an increase in the EF of Pb occurs from a background value of 1.0 (GE9) to a value of 1.9 (GE11). The increase in Pb production between 1870 and 1905 could explain these increased levels of heavy metals (Fig. 5). In terms of the relative chronology, therefore, the geochemical analysis shows that the lower stratigraphic slackwater deposits units (GE1 to GE9) are probably older than 1870. The EF of Pb is higher in the uppermost flood units of the terrace, around 3.3 in GE18 and 10.5 in GE19. The first high EF of 3.3 can be linked to the strong increase of Pb production during the mid-1960s (GE18) and the very high EF of 10.5 to the major pollution of the basin in 1976 (GE19, Fig. 5).

In addition to the trace metal, ^{137}Cs and $^{210}\text{Pb}_{\text{ex}}$ activities as age marker horizons, extreme floods during the last 50 years also produced very prominent stratigraphic horizons. These age controls were combined with the continuous record of stage available from 1890 at the Remoulins gauging station located 15 km downstream (data from SPC 30). The combined records were then used to assign ages to slackwater deposits indicative of other large floods in the GE sequence (Fig. 5). The 1958 event, the second largest in instrumental record ($6400 \text{ m}^3/\text{s}$), deposited a 25-cm-thick unit of medium sands (GE16: $270 \mu\text{m}$). The next three flood units (GE17, GE18, and GE19) are well marked by the pollution of Pb and ^{137}Cs and have been assigned to three lower magnitude floods (4000 , 2900 , and $3000 \text{ m}^3/\text{s}$, respectively) that occurred in 1963, 1969, and

1976, respectively (Fig. 5). Thin sedimentary layers and fine sands characterize these three flood units. The 2002 event, the largest in the instrumental record, deposited a 30-cm- thick unit of medium sands (GE20). From these different flood units, a positive correlation ($r^2=0.96$) exists between the magnitude of the flood versus the grain size/thickness of the different units. The sedimentary flood record prior to 1958 at site GE seems incomplete, as indicated by the fact that fewer post-pollution flood units are preserved (seven units since 1890) than there were flood events with a discharge of sufficient magnitude to cover the sedimentary surface (Fig. 5). Based on the results of the hydraulic model, about 25 flood events would have submerged terrace GE between 1870 ($>1430 \text{ m}^3/\text{s}$) and 1958 ($>1700 \text{ m}^3/\text{s}$) for the scenario for a roughness coefficients K increased by 10% and input flows overestimated by 10% (Figs. 4C and 5). Assuming that a minimum depth of water is required above the site in order for the sediment to deposit in a sufficiently thick layer, it is possible that events of lower magnitudes are not recorded in the sedimentary record. In that case, based on the possible relationship between sediment grain size and magnitude, GE15 could be associated to 1951, GE14 to 1943, GE13 to 1933, GE12 to 1915, GE11 to 1907, GE10 to 1900, and GE9 to 1890 (Fig. 5). Erosion, errors in hydrological documentary sources, and model approximation could also be at the origin of this low correlation between sedimentary flood record and the continuous record of Gardon flow between 1890 and 1958.

Insert Fig. 5 near here

5.1.2. Cave GG

Cave GG is located at 15 m above the channel bed with a minimum estimated discharge of approximately $4500 \text{ m}^3/\text{s}$ required for floodwaters to reach the site (Fig. 4c). Results from the

hydraulic model suggest that at least three events have submerged GG. Cave GG contains more than 1.5 m of slackwater flood sediments. In this article, only the upper 35 cm will be discussed. Six depositional units were found on the first 35 cm, four of which correspond to flood deposits (Fig.6). The flood deposits consist of fine sand to silt, featuring diffused lamination, with many charcoal pieces and ash lens. Median grain size (d₅₀) is clearly affected by the presence of charcoals and ash lens. The ¹³⁷Cs data indicates activity in only one sample analysed in the upper part of the profile (GG4 with a value of 2 mBq/g). The same pattern is observed for ²¹⁰Pb_{ex} activity (Fig. 6). ²¹⁰Pb activity is recorded in the flood unit GG4 (14mBq/g), with no activity in the older deposits. The presence of ¹³⁷Cs activity and ²¹⁰Pb_{ex} activity in this unit means that the age of GG4 post-date 1955 (Fig. 6). At 15 cm depth, a slight increase in the EF of lead occurs (from a background value of 1 to a value of 1.4). The increase production of lead between 1870 and 1905 could explain this increased level of heavy metals occurring in the slackwater deposit GG2 (Fig 6). The EF of lead is higher in the uppermost flood units of the terrace, around 2.2 in GG3 and 4.4 in GG4. The high EF of 2.2 and more in this unit means that the age of GG3 and GG4 post-date the beginning of the twentieth century but cannot be associated to precise ages. The combined records were then used to assign ages to slackwater deposits indicative of other large floods in the GG sequence (Fig. 6). The 1907 event, the third largest in instrumental record (5200 m³/s), deposited a 5-cm- thick unit of fine sands (GG2). The next flood unit, assigned to the second largest in instrumental record (1958:6300 m³/s), deposited a 5-cm- thick unit of fine sands (GG3). The 2002 event, that is the largest in the instrumental record, deposited a 4-cm- thick unit of fine sands (GG4). The 1961 and 1976 events did not reach the cave and may explain why the EF of Pb is not higher than 4.4.

Insert Fig. 6 near here

5.2. Radiocarbon dating

In the fluvial terrace GE, 17 dates were obtained using conventional radiocarbon analysis on wood charcoals and seeds. All of the obtained dates are plotted in Fig. 7 in yBP (corrected for isotopic fractionation) and calibrated to calendar years. From this recent terrace GE, one would normally expect progressively younger dates in the uppermost flood units of the terrace. For radiocarbon analysis on charcoals, at the exception of the first two radiocarbon dates in GE1 (200 yBP) and GE2 (285 yBP), radiocarbon dates are older than expected for the basal part of the terrace GE but considerably older (between 520 and 6540 yBP) than those obtained by the other techniques in the uppermost flood units of the terrace. Uncalibrated ^{14}C ages of seeds are often in an inverted stratigraphic position. However, when these ages are calibrated at 2σ they are consistent with those obtained by the other dating techniques.

Insert Fig. 7 near here

6. Discussion

6.1. Dating techniques

Ages for modern flood deposits have been correctly assigned with the use of ^{137}Cs . The presence or absence of ^{137}Cs in these flood deposits of the Gardon River is not controlled by the particle size distribution. In the upper four deposits (units 17 through 20), ^{137}Cs was detected even in the

sample with the lowest clay content ($F < 2\mu\text{m}: 0.03\%$) (Fig. 5). Moreover, the uppermost pre-bomb deposit (unit 15) showed no ^{137}Cs activity. There was no leaching of ^{137}Cs into the post-bomb deposits from the overlying post-bomb deposits, as no samples below unit 16 showed detectable ^{137}Cs . Four samples from the flood deposit G20 (2002) showed ^{137}Cs activity, although atmospheric ^{137}Cs fallout is negligible during this period. The presence of ^{137}Cs in this recent flood deposit could have resulted from the erosion and redeposition of post-1950 floodplain or terrace deposits. Our results are consistent with other authors (Ely et al., 1992; Thorndycraft et al., 2005a,b), who found that (i) ^{137}Cs is concentrated by erosion and redeposition of fine-grained sediments and (ii) significant ^{137}Cs activity in sandy sediments indicates that high clay content is not necessary for this method to be effective in distinguishing pre- and post-1950 deposits.

The $^{210}\text{Pb}_{\text{ex}}$ confirms a number of results produced using the ^{137}Cs dating technique. The high $^{210}\text{Pb}_{\text{ex}}$ activity recorded in flood units GE19 and its exponential decrease in the other flood deposits (GE18 to G15) suggests that the uppermost part of the terrace is recent (< 100 years, i.e., ~ 4 to 5 times its decay period of 22.3 years) and can be considered as being stratigraphically undisturbed. Significant $^{210}\text{Pb}_{\text{ex}}$ activity in sandy sediments indicates that high clay content is also not necessary for this method to be used. However, without clay-normalized absorbed $^{210}\text{Pb}_{\text{ex}}$ activity and without using a model of ^{210}Pb input during floods, this approach is not sufficiently accurate for dating episodic sediment accumulation on terraces (Aalto and Nittrouer, 2013).

Ages for modern flood deposits have been correctly assigned with the use of lead generated by mining activity. The latest sediment deposit GE20 (2002) presents EF of lead similar to those of 1969. This latest sedimentary deposit (GE20) might reflect remobilization of ancient floodplain sediments, acting as a secondary contamination source during large flood events. However, the similarity of EF values in the 2002 flood deposit and in current stream sediments (E. Resongles,

HSM, personal communication, 2014), rather points out limited improvement of sediment quality by waste water treatment over recent years. Interestingly, the values of EF of Pbin units GG3 and GG4 (1958 and 2002 events in cave GG) are the same that in the equivalent flood event in the sequence GE16 and GE20 (1958 and 2002 events in terrace GE). This would suggest that each flood event is characterized by an EF of Pb. This result also means that the EF ratio of Pbis not controlled by the particle size distribution. If this is confirmed in later studies, EF of Pbcould be used as another proxy for dating flood deposits in this study area.

Eighty percent of dates on charcoal samples are much older than is reasonably expected (Fig. 7). In the GE terrace, the prevailing inversion of dates, with many of these recording ages older than expected, is most likely a response to remobilization of sediment. The Gardon River does not transport material downslope in direct fashion from upstream source areas to our study site during a single, rapid flood event, but rather in a process that comprises several episodic floods, small channel migration events on the Gard plain between the Alès graben and Gardon gorges is envisioned. During extreme flood events, the inundated area is considerably increased and may cover a part of the old terraces. Sediment is temporarily stored until it is exposed by small channel migration or erosion of old terraces, mobilized and then once again redeposited. Other processes may affect the radiocarbon dating techniques on charcoals such as alteration of samples, by percolation, infiltration from underlying sections (Evans, 1985; Tornqvist et al., 1998), or hardwater effect (a term for the old-carbon reservoir derived from dissolved carbonate rocks; Saarnisto, 1988). Sediments of large flood deposits in GE and GG contain a high proportion of quartz, (>45%), illite/mica (>45%),and relatively little carbonate or dolomite (<3%). These minerals present in flood deposits derive mainly from the erosion of Paleozoic granite, schist, and gneiss rocks in the upper part of the Gardon drainage basin. Charcoals have probably the same origin, i.e.,coming from the combustion of treesthatinitially livedin the

Cévennes Mountains. Thus, consistent with the origin of the sediment, our radiocarbon dates do not have a significant hardwater error, i.e., not initially affected by an oldcarbon reservoir. Another possible explanation lies in the industrial past of the study area. The Gardon watershed presents numerous coal mines, which were extensively exploited during the nineteenth and twentieth centuries. The sediment of terrace GE contains a high proportion of small graphite particles (~ 80% of the carbon material in the different flood units sieved). Therefore, it can also be suggested that the binding of small particles of dead carbon on the charcoal produce an aging of the ^{14}C ages. We estimated the induced aging process by adding 10% of a dead carbon on a charcoal dated to 1950. Ten percent is a relatively high value. In this case, this charcoal would have an age of 1079 years AD ($1950 - t_{\text{modern } ^{14}\text{C with 10\% of dead carbon}} = 1950 - \ln(100/90) \cdot 8266.6$), which cannot explain the results of the radiocarbon dating on charcoals. To conclude, all these other processes alone may not account for the extremely wide range in age offset and chronologic error; and the remobilization of sediment is probably the first process, which can affect our radiocarbon dates.

Radiocarbon dating on seeds seems to give better results. Almost two reasons may explain this dating difference between charcoal and seeds. Firstly, the seed is an annual product of a living plant when charcoal is produced by incomplete combustion of a living or dead tree/shrub, possibly very old. This effect is called ‘inbuilt age’ or ‘old wood effect’ (Gavin, 2001) because woody plants maintain old tissues in their structure; branches and stems could be greatly older than the date of the fire event and even more than the flood event. Thus the ^{14}C date of a charcoal might be significantly older than a ^{14}C date of a seed in the same flood unit. Secondly, charcoals are relatively large and decay-resistant, they are likely to remain in the vicinity of the riverbank a longer time than smaller and more readily decomposed seeds (Oswald et al., 2005). At site GE, the seeds probably have a local origin. The identified seeds are essentially *Polycnemum*, *Carex*,

Sambucus ebulus, and *Medicago*, which grow presently on the riverbank. However, although dating of seeds provides better results than charcoal, the accuracy of this technique is limited because of the large uncertainty of the ^{14}C dates compared to discrete flood events. Only the combined use of ^{210}Pb , ^{137}Cs and geochemical analysis of mining-contaminated sediments with the instrumental flood record can be applied to discriminate and date the recent slackwater deposits of the terrace GE and cave GG.

6.2. Uncertainties affecting record completeness

The principal goal of a typical slackwater paleoflood investigation is to enumerate floods represented in the stratigraphic record as accurately and completely as possible and to determine their timing as precisely as possible (Kochel and Baker, 1988). This task is influenced by several types of uncertainty, which include the effects of stratigraphic ambiguity, erosion, internal stratigraphic complexity, incomplete exposure, pedogenesis, stratigraphic record self-censoring (House et al., 2002), and the uncertainties for dating slackwater flood sediments. Taking into account these effects have important implications for evaluating the information content of regional or site-specific fluvial paleoflood data. The stratigraphic records of GE and GG are excellent examples to illustrate the effects of erosion/preservation in a context of a progressively self-censoring vertically accreting sequence. The sedimentary flood record between 1958 and 2010 at site GE seems complete. Prior to 1958, this record is incomplete, as indicated by the fact that fewer post-pollution flood units (seven units) are preserved than there were flood events with a discharge of sufficient magnitude to cover the sedimentary surface (25 events approximately). As suggested, the most likely cause of this incomplete record is erosion. The second largest flood on record was that of 1958; however, the stratigraphy suggests that this event was not responsible for the erosion of earlier deposits. The contact between units GE15 and GE16 is characterized by

buried soils, and no evidence of an erosive contact is observed. It is likely, therefore, that the sedimentary record reflects a change in preservation potential of the sediments as distinct from the erosive capability of a particular flood. During the 78-year period 1880-1958, 25 floods of a sufficient magnitude ($> 1450 \text{ m}^3/\text{s}$) have covered the terrace. Since 1958, however, the frequency of inundation of the deposits has been lower, there have only been five or six floods in 52 years large enough to exceed the necessary threshold discharge ($> 1700 \text{ m}^3/\text{s}$). The progressive increase of threshold discharge and the reduced frequency of inundation at the terrace could allow stabilisation of the vegetation cover and improved protection against erosion from subsequent large magnitude flood events (the extreme 2002 event has not eroded the buried soils of the 1976 event). A high frequency of events would not have enabled such a high degree of stabilisation, rendering the deposits more susceptible to erosion. In cave GG located 15 m above the channel bed, the sedimentary flood record between 1907 and 2010 seems complete, as indicated by the fact that there are as many post-pollution flood units (three units) preserved as flood events with a discharge of sufficient magnitude to cover the sedimentary surface (three events: 1907, 1958, and 2002). Here, the low frequency of events would have enabled a high degree of stabilisation of the sedimentary flood record, rendering the deposits less susceptible to erosion. This higher stabilisation is also probably facilitated by a strong decrease of the flood current velocity in this cave. To conclude, at low elevation sites, frequent flooding may erode the slackwater flood sediments (e.g., the lower part of terrace GE). In contrast, deposits in high elevation caves or terraces (largest floods) may have a larger preservation potential, since only extreme events are able to flush away the sediments accumulated at these higher sites. These observations are not new. They have been stated previously in the paleoflood literature with varying degrees of emphasis (House et al., 2002; Thorndycraft et al., 2005a,b). However, our study in the Gardon River illuminated several types of uncertainties and suggested several others with an excellent

example to illustrate the effects of erosion/preservation in a context of a progressively self-censoring, vertically accreting sequence.

6.3. Relation to other paleoflood records in the region

Sheffer et al. (2008) described a series of 10 distinct slackwater deposits in a cave 12 m above the river bed (cave GH) at 400 m downstream of the GE site. From this cave, Sheffer et al. (2008) deduced an increase of flood events during the Little Ice Age and to a cold and wet phase around 2850 years ago. This is an important result because it allowed us to highlight a link between flood events and climate variability at the regional and southern European scale. Cave GH is located at an elevation below the 2002 flood water level representing low magnitude floods, and slackwater deposits matched a minimum associated discharge of 2600 m³/s. Cave GH contains at least seven units deposited in the last 2000 years (Sheffer et al., 2008). Assuming a minimum discharge of 2600 m³/s, the upper part of this cave should record at least eight flood events during the twentieth century and not only seven during the last 2000 years. This discrepancy could be related to erosion because of the low position of the cave or to erroneous radiocarbon dates. As observed in terrace GE where 80% of dates on charcoal samples are much older than is reasonably expected, radiocarbon ages on charcoal samples of slackwater deposits in cave GH could also be erroneous in the uppermost part of this cave. To conclude, a supplementary geochronological study of this alluvial sequence would be necessary to confirm or not these first palaeohydrological results of Sheffer et al. (2008).

8. Conclusion

Our detailed paleoflood investigation on the Gardon River has shown some strengths and weaknesses of slackwater paleoflood hydrology as a technique for improving understanding of the frequency of floods in bedrock channels. ^{210}Pb , ^{137}Cs , and geochemical analysis of mining-contaminated sediments have been used to reconstruct the history of slackwater flood deposits. This approach was combined with the continuous record of Gardon water levels since 1890 to assign ages to slackwater deposits. At cave GG and fluvial terrace GE, respectively located at 15 and 10 m above the channel bed, these dating techniques have been successfully applied and illustrate the potential of this multidating approach in dating recent slackwater flood deposits. The sedimentary flood record was complete in cave GG but not in terrace GE. We deduced that at low elevation sites, frequent flooding could erode the slackwater flood sediments (e.g., the lower part of terrace GE). In contrast, deposits in high elevation caves or terraces (largest floods) could have a larger preservation potential, as only extreme events were able to flush away the sediments accumulated at these higher sites.

Most ^{14}C dates on wood charcoal samples (80%) in the terrace GE were much older than the age reasonably expected. In the terrace, the prevailing inversion of dates, with so many of these recording ages older than expected, was most likely a clear response to fluvial remobilization of sediment and their organic contents. Radiocarbon dating on seeds seems to give better results and could be explained by an absence of ‘inbuilt age’ effect and low decay-resistance compared to wood charcoals. However, although the dating of seeds provides better results than wood charcoal, the accuracy of this technique is limited to date flood events from the most recent centuries. Only the combined use of ^{210}Pb , ^{137}Cs , and geochemical analysis of mining-

contaminated sediments with the instrumental flood record can be applied to discriminate and date the recent slackwater deposits of the terrace GE and cave GG.

Acknowledgements

This project was totally funded by the ANR commission (EXTRAFLO project). The authors wish to thank Thierry Montecinos, Marie Bouchet, Stéphanie Garnero, Isabelle Avril, Cyril Soustelle, Neri for their help in fieldwork; the IRSTEA team for doing bathymetric cross sections; the DDE Nîmes for the historical flood data; Laurent Bouby for seeds identifications. We thank the Laboratoire de Mesure ^{14}C (LMC14) ARTEMIS in the CEA Institute at Saclay (French Atomic Energy Commission) for the ^{14}C analyses (EXTRAFLO project). We thank the three anonymous reviewers for their constructive comments on the manuscript.

References

- Aalto, R., Nitttrouer, C., 2012. 210Pb geochronology of flood events in large tropical river systems. (2012). *Phil. Trans. R. Soc. A* 370, 2040–2074.
- Appleby, P. G., Oldfield, F., 1978. The calculation of Pb-210 dates assuming a constant rate of supply of unsupported Pb-210 to the sediment. *Catena* 5, 1–8.
- Appleby, P., Oldfield, F., 1992. Application of lead-210 to sedimentation studies. In: Ivanovich, M., Harmon, R.S., (Eds.), *Uranium Series Disequilibrium, Application to Earth, Marine and Environmental Sciences*. Clarendon Press, Oxford, UK, pp. 773–778.
- Atwater, B.F., Trumm, D.A., Tinsley, J.D., III, Stein, R.S., Tucker, A.B., Donahue, D.J., Jull, A.J.T., Payen, L.A. 1990. Alluvial plains and earthquake recurrence at the Coalinga anticline. In Rymer, M.J., Ellsworth, W.L. (Eds.), *The Coalinga, California, Earthquake of May 2, 1983*. Publisher City, ST, pp. 273–297, 1487.
- Baker, V.R., 1987. Paleoflood hydrology and extraordinary flood events. *Journal of Hydrology*

96, 79–99.

Baker, V.R., Kochel, R.C., 1988. Flood sedimentation in bedrock fluvial systems. In: Baker, V.R., Kochel, R.C., Patton, P.C. (Eds.), *Flood Geomorphology*. Wiley, city,USA, pp. 123–137.

Baker, V.R., Webb, R.H., House, P.K., 2002. The scientific and societal value of paleoflood hydrology. In: House, P.K., Webb, R.H., Baker, V.R., Levish, D.R. (Eds.), *Ancient Floods, Modern Hazards: Principles and Applications of Paleoflood Hydrology*. Water Science and Application Series, vol. 5, AGU, Washington, DC, pp. 127–146.

Benito, G., Sopena, A., Sanchez, Y., Machado, M.J., Perez Gonzalez, A., 2003a. Palaeoflood record of the Tagus River (central Spain) during the late Pleistocene and Holocene. *Quaternary Science Reviews* 22, 1737–1756.

Benito, G., Sanchez-Moya, Y., Sopena, A., 2003b. Sedimentology of high-stage flood deposits of the Tagus River, central Spain. *Sedimentary Geology* 157, 107–132.

Benito, G., Lang, M., Barriendos, M., Llasat, M.C., Frances, F., Ouarda, T., Thorndycraft, V.R., Enzel, Y., Bardossy, A., Coeur, D., Bobee, B., 2004. Use of systematic, palaeoflood and historical data for the improvement of flood risk estimation. Review of scientific methods. *Nat. Hazards* 31, 623–643.

Benito, G., Thorndycraft, V.R., 2005. Palaeoflood hydrology and its role in applied hydrological sciences. *Journal of Hydrology* 313, 3–15.

Bonnifait, L., Delrieu, G., Le Lay, M., Boudevillain, B., Masson, A., Belleudy, P., Gaume E., Saulnier, G.-M., 2009. Hydrologic and hydraulic distributed modelling with radar rainfall input: reconstruction of the 8-9 September 2002 catastrophic flood event in the Gard region, France. *Advances in Water Resources* 32, 1077–1089.

Bonté, P., Ballais, J.L., Masson, M., Ben Kehia, H., Eyraud, C., Garry, G., Ghram, A., 2001. Datations au ¹³⁷Cs, ¹³⁴Cs et ²¹⁰Pb de dépôts de crues du XXe siècle. *Datation, XXIe rencontres internationales d'archéologie et d'histoire d'Antibes*, Ed. APDCA, 141–157.

Cremers, A., Elsen, A., De Preter, P., Maes, A. 1988. Quantitative analysis of radiocaesium retention in soils. *Nature* 335, 247–249.

Davies, B.E., Lewin, J., 1974. Chronosequences in alluvial soils with special reference to historic lead pollution in Cardiganshire, Wales. *Environ Pollut* 6, 49–57.

DREAL, 2008. Internet site: <http://basol.developpement-durable.gouv.fr/>

- 694 El kadi Abderrezzak, K., Paquier, A., 2009. One-dimensional numerical modeling of sediment
695 transport and bed deformation in open channels. *Water Resour. Res.* 45, W05404.
- 696 Elbaz-Poulichet, F., Bruneel, O., Casiot, C., 2006. The Carnoules mine. Generation of As-rich
697 acid mine drainage, natural attenuation processes and solutions for passive in-situ
698 remediation. *Documentation IRD*, p 1–8.
- 699 Ely, L.L., Baker, V.R., 1985. Reconstructing paleoflood hydrology with slackwater deposits
700 Verde River, Arizona. *Physical Geography* 6, 103–126.
- 701 Ely, L.L., Webb, R.H., Enzel, Y., 1992. Accuracy of post-bomb ^{137}Cs and ^{14}C in dating fluvial
702 deposits. *Quaternary Research* 38, 196–204.
- 703 Enzel, Y., Ely, L.L., Martinez, J., Vivian, R.G., 1994. Paleofloods comparable in magnitude to
704 the catastrophic 1989 dam failure flood on the Virgin River, Utah and Arizona. *Journal of*
705 *Hydrology* 153, 291–317.
- 706 Evans, L.J., 1985. Dating methods of Pleistocene deposits and their problems. VII. Paleosols.
707 In:ed. Rutter, N.W. (Ed.), *Dating Methods of Pleistocene Deposits and Their Problems*. Repr.
708 Ser. Geosci. Canada, Toronto, Canada, pp. 53–59.
- 709 Gavin, D.G., 2001. Estimation of inbuilt age in radiocarbon ages of soil charcoal for fire history
710 studies. *Radiocarbon* 43, 27–44.
- 711 Golberg E., 1963. Geochronology with ^{210}Pb . *Radioactive Dating*. International Atomic
712 Energy Agency, Vienna, Austria, pp. 121–31.
- 713 He, Q., Walling, D.E., 1996. Interpreting particle size effects in the adsorption of ^{137}Cs and
714 unsupported ^{210}Pb by mineral soils and sediments. *J. Environ. Radioact* 30, 117–137.
- 715 Hindel, R., Schlich, J., De Vos, W., Ebbing, J., Swennen, R., Van Keer, Y., 1996. Vertical
716 distribution of elements in overbank sediment profiles from Belgium, Germany and The
717 Netherlands. *Journal of Geochemical Exploration* 56, 105–122.
- 718 House, P.K., Pearthree, P.A., Klawon, J. E., 2002. Historical Flood and Paleoflood Chronology
719 of the Lower Verde River, Arizona: Stratigraphic Evidence and Related Uncertainties. In :
720 House, P. K., Webb, R. H., Baker, V. R., Levish D. R., (Eds.), *Ancient Floods, Modern*
721 *Hazards*, American Geophysical Union, Washington, D.C., pp. 267–293.
- 722 Huet, P.X., Martin, J.L., Prime, P., Foin, C., Laurain, P., Cannard, 2003. Retour d'expérience
723 décrues de septembre 2002 dans les départements du Gard, de l'Hérault, du Vaucluse, des
724 Bouches du Rhône, de l'Ardeche et de la Drome. *Rapport de l'Inspection Générale de*

l'Environnement. Ministre de l'Ecologie et du Développement Durable, République Française. 133 pp. Available at the Internet site: <http://www.environnement.gouv.fr/infoprat/Publications/publi-ige.htm>.

Knox, J.C., Daniels, J.M., 2002. Watershed scale and the stratigraphic record of large floods. In : House, P. K., Webb, R. H., Baker, V. R., Levish, D. R., (Eds.), *Ancient Floods, Modern Hazards*, American Geophysical Union, Washington, D.C., pp. 237–255.

Kochel, R.C., Baker, V.R., Patton, P.C., 1982. Palaeohydrology of southwest Texas. *Water Resour. Res.* 18, 1165–1183.

Kochel, R.C., Baker, V.R., 1988. Paleoflood analysis using slack water deposits. In: Baker, V.R., Kochel, R.C., Patton, P.C. (Eds.), *Flood Geomorphology*. John Wiley and Sons, U.S.A., pp. 357–376.

Lewin, J., Davies, B.E., Wolfenden, P.J., 1977. Interaction between channel change and historic mining sediments. In K.J. Gregory (Ed.), *River channel changes*, pp. 353–367.

McHenry, J.R., Ritchie, J.C., 1977. Physical and chemical parameters affecting transport of ^{137}Cs in arid watersheds. *Water Resources Research* 13, 923–927.

Nuissier, O., Ducrocq, V., Ricard, D., Lebeaupin, C., Anquetin, S., 2008. A numerical study of three catastrophic precipitating events over southern France. I : Numerical framework and synoptic ingredients. *Quart. J. Roy. Meteor. Soc.* 134, 111–130.

Nydal, R., Lovseth, K., 1983. Tracing bomb ^{14}C in the atmosphere 1962–1980. *Journal of Geophysical Research* 88, 3621–3642.

Oswald, W.W., Anderson, P.M., Brown, T.A., Brubaker, L.B., Hu, F.S., Lozhkin, A.V., Tinner, W., Kaltenrieder, P., 2005. Effects of sample mass and macrofossil type on radiocarbon dating of arctic and boreal lake sediments. *The Holocene* 15, 758–767.

Popp, C. J., Hawley, J. W., Love, D. W., Dehn, M., 1988. Use of radiometric (^{137}Cs , ^{210}Pb), geomorphic, and stratigraphic techniques to date recent oxbow sediments in the Rio Puerto Drainage. Grants Uranium Region, New Mexico. *Environmental Geology and Water Science* 3, 253–269.

Ritchie, J.C., McHenry, J.R., Gil, A.C., 1974. Fallout ^{137}Cs in the soils of three small watersheds. *Ecology* 55, 887–890.

Saarnisto, M., 1988. Time-scales and dating. In: Huntley, B., Webb, T. (Eds.), *Vegetation History. Handbook of vegetation science*. Kluwer Academic Publishers, Dordrecht, pp. 77–

- 112.
- SAGE des Gardons, 2000. Annexe 1 au Schéma d'Aménagement et de Gestion des Eaux des gardons, SAGE, pp 187.
- Sheffer, N.A., Rico, M., Enzel, Y., Benito, G., Grodek, T., 2008. The palaeoflood record of the Gardon River, France: A comparison with the extreme 2002 flood event. *Geomorphology* 98, 71–83.
- Springer, G.S., 2002. Caves and their potential use in paleoflood studies. In: House, P.K., Webb, R.H., Baker, V.R., Levish, D.R. (Eds.), *Ancient Floods, Modern Hazards: Principles and Applications of Paleoflood Hydrology*. Water Science and Applications, AGU, pp. 329–344.
- Stokes, S., Walling, D.E., 2003. Radiogenic and isotopic methods for the direct dating of fluvial sediments. In: Kondolf, M., Piegay, H. (Eds.), *Tools in Fluvial Geomorphology*. Wiley, Chichester, pp. 233–267.
- Stuiver, M., Reimer, P.J., 1993. Extended 14C data base and revised CALIB 3.0 14C age calibration program. *Radiocarbon* 35, 1, 215–30.
- Sutherland, R.A., 1989. Quantification of accelerated soil erosion using the environmental tracer Caesium-137. *Land Degradation and Rehabilitation* 1, 199–208.
- Thorndycraft, V.R., Benito, G., Rico, M., Sopena, A., Sánchez-Moya, Y., Casas-Planes, A., 2004a. A Late Holocene Paleoflood record from slackwater flood deposits of the Llobregat River, NE Spain. *Journal Geological Society of India* 64 (4), 549–559.
- Thorndycraft, V., Brown, A.G., Pirrie, D., 2004b. Alluvial records of Medieval and prehistoric tin mining on Dartmoor, SW England. *Geoarchaeology*, 19, 219–236.
- Thorndycraft, V., Benito, G., Rico, M., Sopena, A., Sánchez-Moya, Y., Casas, A., 2005a. Paleoflood hydrology of the Llobregat River, NE Spain: a 3000year record of extreme floods. *Journal of Hydrology* 313 (1-2), 16–31.
- Thorndycraft, V.R., Benito, G., Walling, D.E., Sopena, A., Sanchez-Moya, Y., Rico, M., Casas, A., 2005b. Caesium-137 dating applied to slackwater flood deposits of the Llobregat River, N.E. Spain. *Catena* 59, 305–318.
- Tisnérat-Laborde, N., Poupeau, J.J., Tannau, J.F., Paterne, M., 2001. Development of a semiautomated system for routine preparation of carbonate samples. *Radiocarbon* 43, 299–304.
- Törnqvist, T.E., Van Ree, M.H.M., Van't Veer R., Van Geel B., 1998. Improving methodology

- for high-resolution reconstruction of sealevel rise and neo-tectonics and paleoecological analysis and AMS 14C dating of basal peats. *Quat. Res.* 49, 72–85
- Trumbore, S.E., 2000. Radiocarbon geochronology. In: Noller, J.S., Sowers, J.M., Lettis, W.R. (Eds.), *Quaternary Geochronology: Methods and Applications*. AGU, Washington, D.C., pp. 41–60.
- Walling, D.E., He, Q., 1997. Use of fallout 137Cs in investigations of overbank sediment deposition on river floodplains. *Catena* 29, 263–282.
- Webb, R.H., Jarrett, R.D., 2002. One-dimensional estimation techniques for discharges of paleofloods and historical floods. In: House, P.K., Weeb, R.H., Baker, V.R., Levish, D.R. (Eds.), *Ancient Floods, Modern Hazards: Principles and Applications of Paleoflood Hydrology*. Water Resources Monograph, vol. 5. AGU, Washington, D.C., pp. 111–12.

List of figures and table

Fig. 1: Topography, hydography, and geological maps of the Gardon river watershed.

Fig. 2: Annual maximum gage height available at Remoulins between 1890 and 2010.

Fig. 3: (A) A map showing the study sites in the Gardon Gorges. (B) Terrace (GE) and cave (GG), sites of slackwater flood sediment archives .

Fig. 4 (A) Cross sections of the paleosites used in the model; (B) Calculated stage-discharge relationships and their envelope and (C) Historical flood series at Remoulins.

Fig. 5. The proposed chronology for the terrace GE slackwater flood deposits, d_{50} , ^{137}Cs activities, $^{210}\text{Pb}_{\text{ex}}$ activities, EF of lead, the peak annual instantaneous discharges series at Remoulins. The envelope on the range of discharges at Remoulins that may have submerged the site resulting from the sensitivity analysis is shown. The individual slackwater flood units deposited by a particular event are annotated.

Fig. 6. The proposed chronology for the cave GG slackwater flood deposits, d_{50} , ^{137}Cs activities, $^{210}\text{Pb}_{\text{ex}}$ activities, the peak annual instantaneous discharges series at Remoulins. The envelope on the range of discharges at Remoulins that may have submerged the site resulting from the sensitivity analysis is shown. The individual slackwater flood units deposited by a particular event are annotated.

Fig. 7. Stratigraphy and age model of site GE. Radiocarbon ages on wood charcoals (in blue) and seeds (in red) in BP and calendar ages (2σ)

Table 1. Results from radiocarbon dating. All calibrated ages were calculated within 2σ . Calibration was carried out using CALIB 6.1.0. The age model integrates the minimum and the maximum value of the calibrated age.

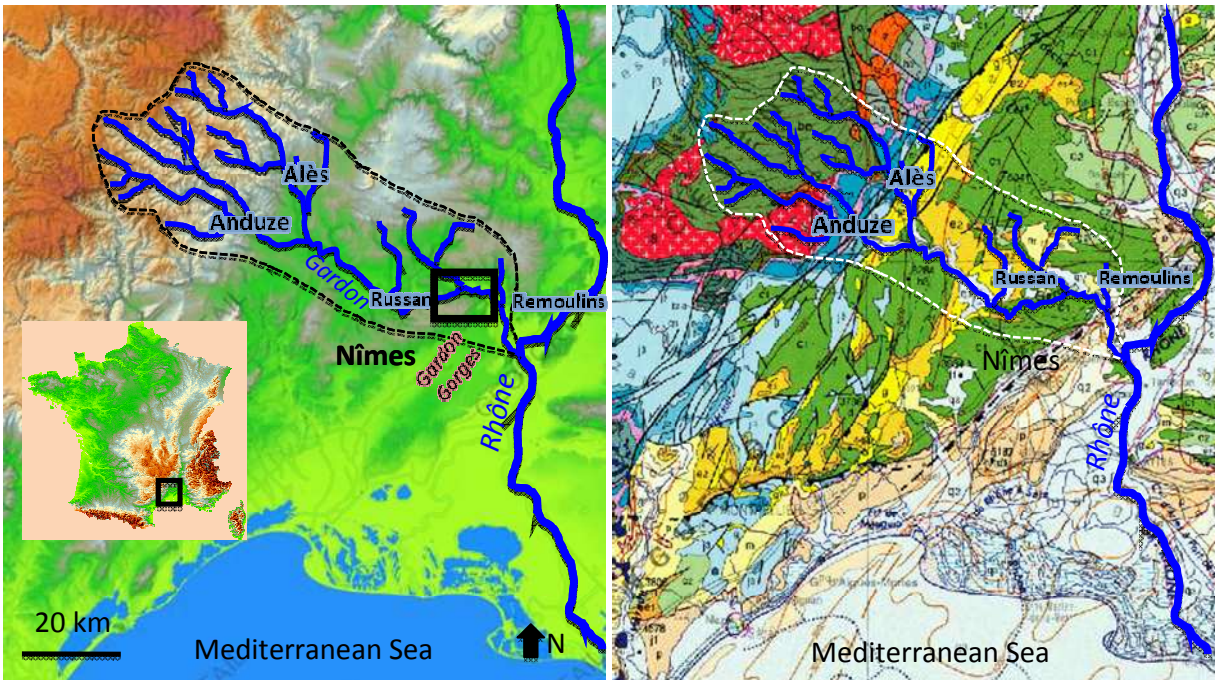


Fig. 1: Topography, hydrography, and geological maps of the Gardon river watershed.

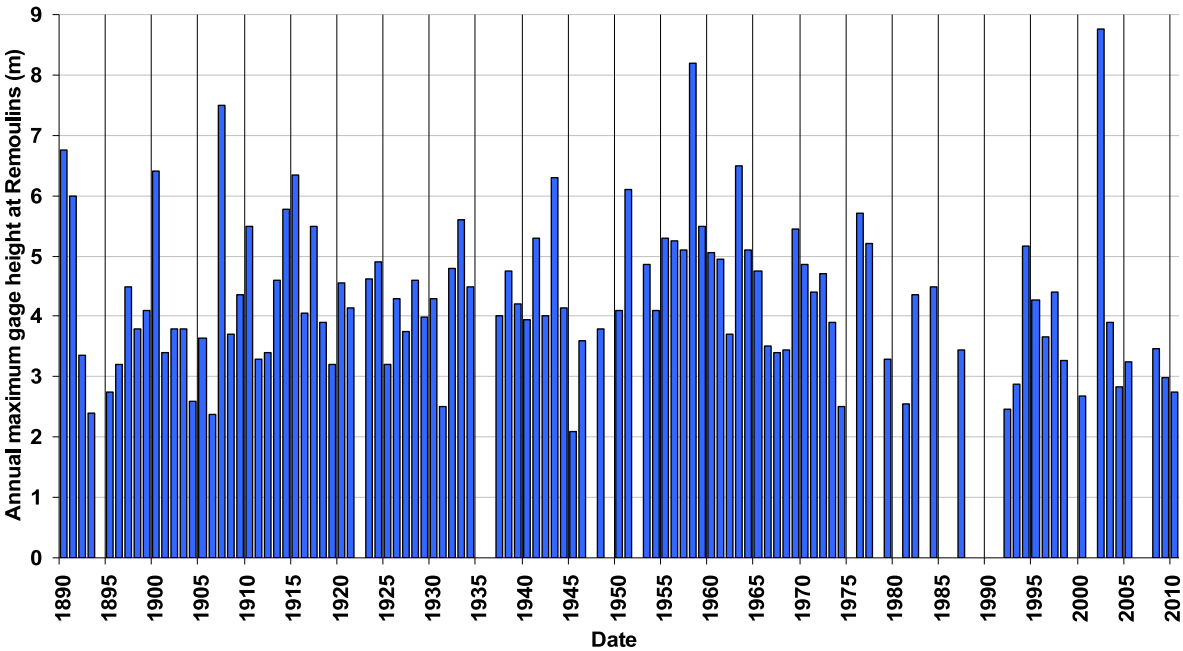


Fig. 2: Annual maximum gage height available at Remoulins between 1890 and 2010.

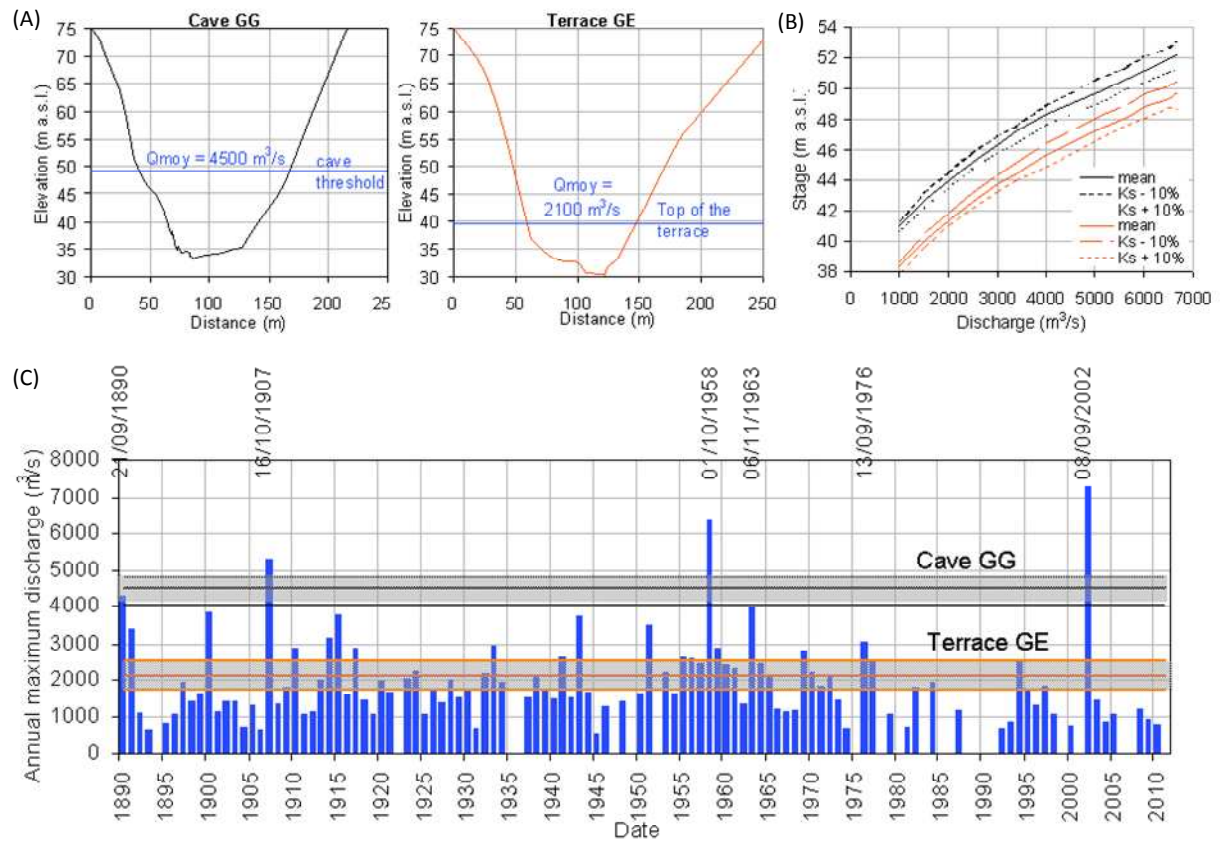
(A)



(B)



Fig. 3: (A) A map showing the study sites in the Gardon Gorges. (B) Terrace (GE) and cave (GG), sites of slackwater flood sediment archives .



841 Fig. 4 (A) Cross sections of the paleosites used in the model; (B) Calculated stage-discharge
842 relationships and their envelope and (C) Historical flood series at Remoulins.

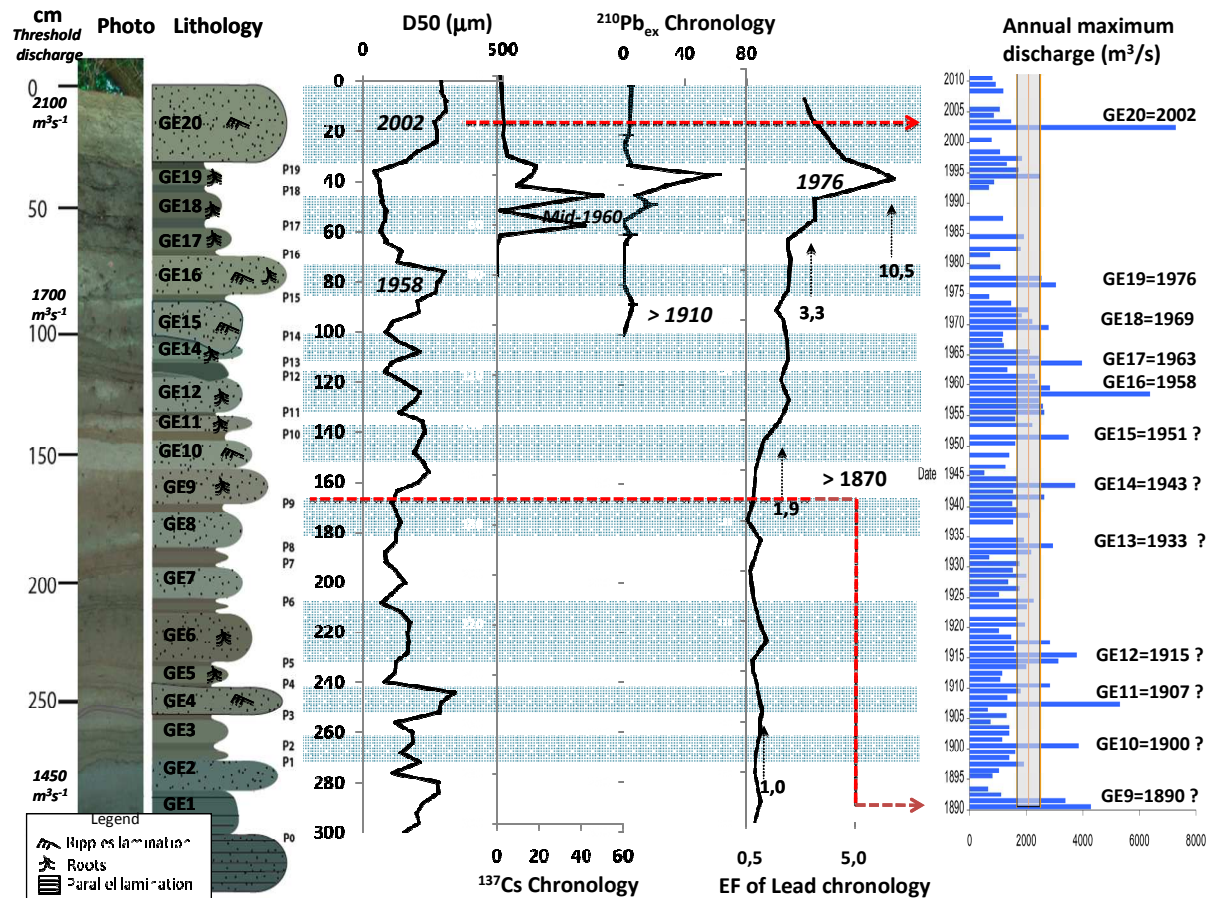
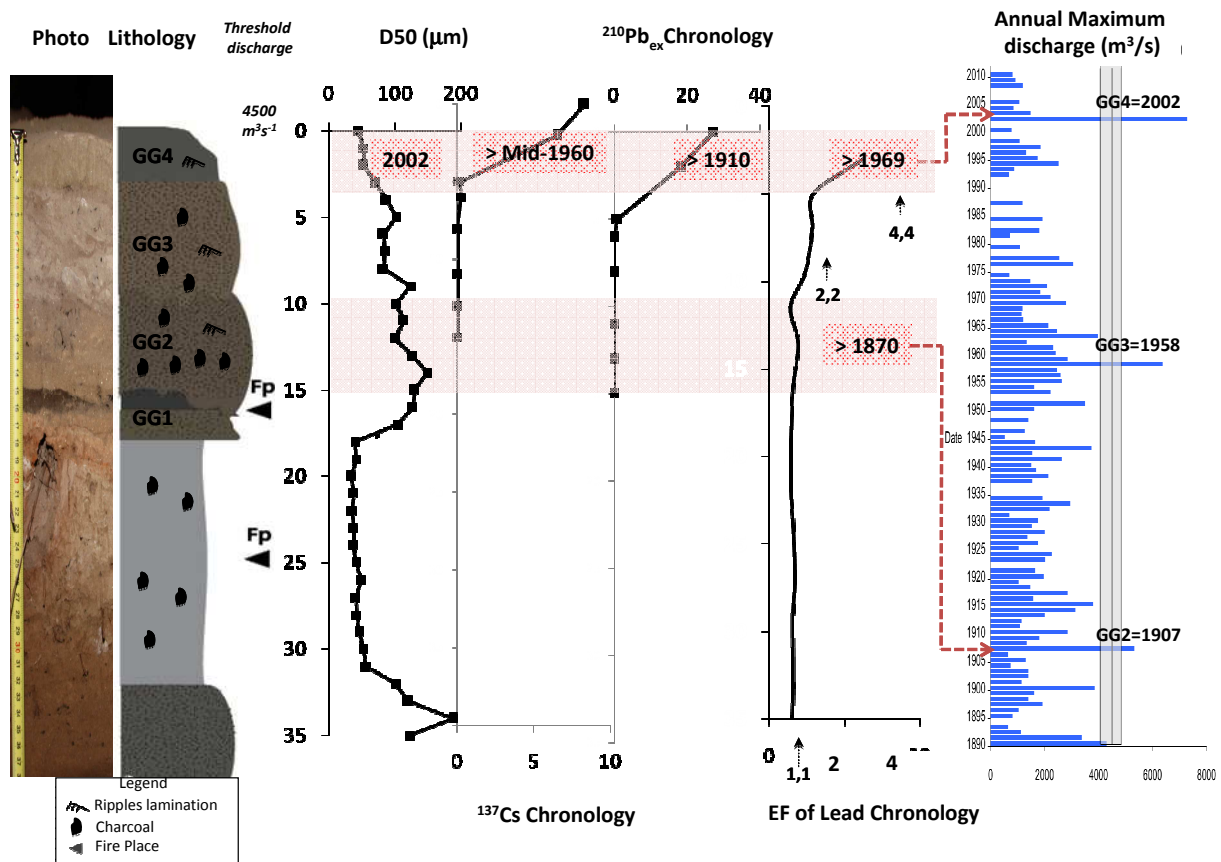


Fig. 5. The proposed chronology for the terrace GE slackwater flood deposits, d50, ¹³⁷Cs activities, ²¹⁰Pb_{ex} activities, EF of lead, the peak annual instantaneous discharges series at Remoulins. The envelope on the range of discharges at Remoulins that may have submerged the site resulting from the sensitivity analysis is shown. The individual slackwater flood units deposited by a particular event are annotated.



848 Fig. 6. The proposed chronology for the cave GG slackwater flood deposits, d50, ^{137}Cs activities,
849 $^{210}\text{Pb}_{\text{ex}}$ activities, the peak annual instantaneous discharges series at Remoulins. The envelope on
850 the range of discharges at Remoulins that may have submerged the site resulting from the
851 sensitivity analysis is shown. The individual slackwater flood units deposited by a particular
852 event are annotated.

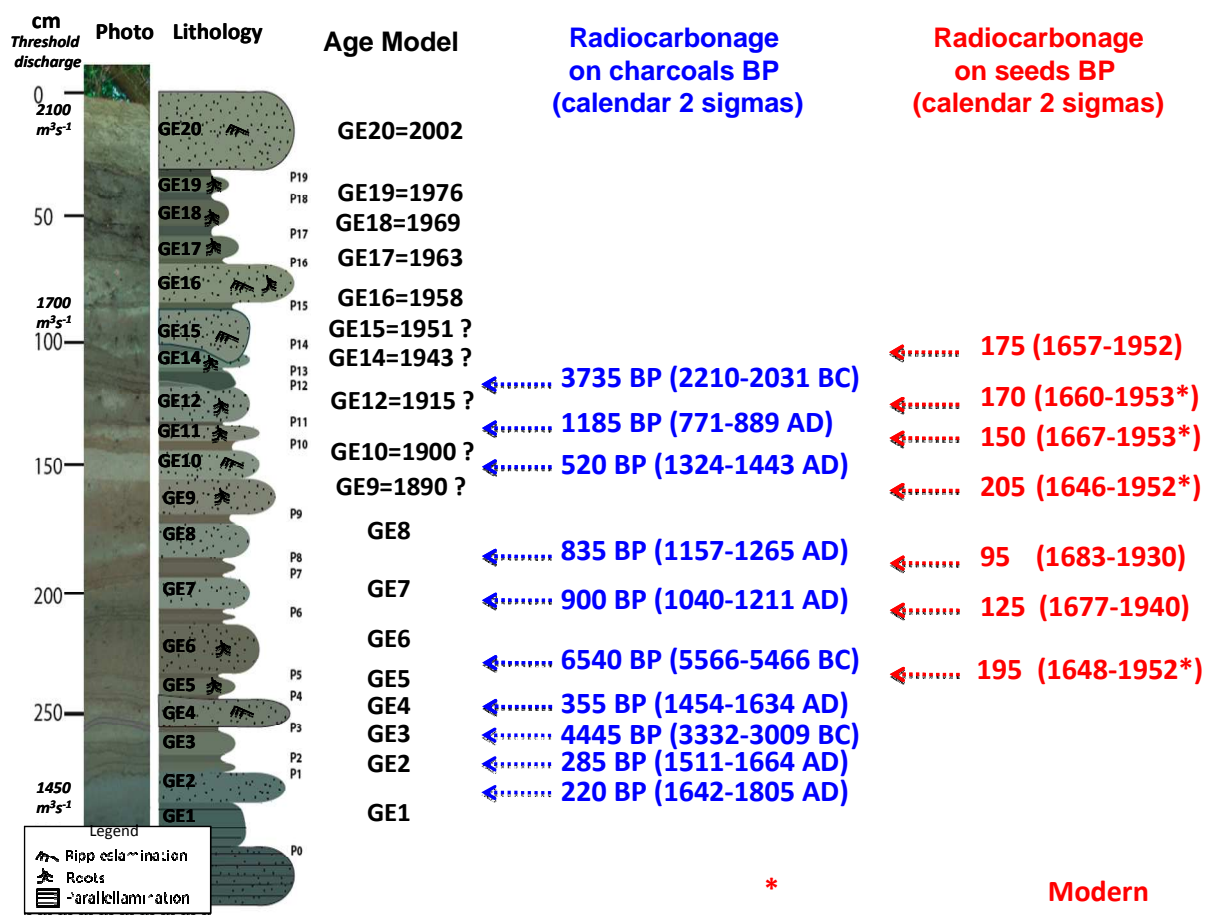


Fig. 7. Stratigraphy and age model of site GE. Radiocarbon ages on wood charcoals (in blue) and seeds (in red) in BP and calendar ages (2σ)

857 Table 1. Results from radiocarbon dating. All calibrated ages were calculated within 2σ .
858 Calibration was carried out using CALIB 6.1.0. The age model integrates the minimum and the
859 maximum value of the calibrated age.

Sample	Type	Age	Calibrated age (agreement % Age model)	
GE113-116	charcoal	3735± 35	2210-2031 BC (94%)	2210-2031 BC
GE 132-135	charcoal	1185±30	771-899 AD (92%)	771-899 AD
GE 148-152	charcoal	520±30	1324 1345 AD (10%) 1393-1443 AD (89%)	1324-1443 AD
GE 192-195	charcoal	835±30	1157-1265 AD (100%)	1157-1265 AD
GE 208-214	charcoal	900±30	1040-1110 AD (44%) 1115-1211 AD (55%)	1040-1211 AD
GE 238-243	charcoal	6540±40	5566-5466 BC (92%)	5566-5466 BC
GE 257-262	charcoal	355±35	1454-1529 AD (47%) 1540-1634 AD (53%)	1454-1634 AD
GE 267-270	charcoal	4445±35	3332-3213 BC (38%) 3132-3009 BC (51%)	3332-3009 BC
GE 275-280	charcoal	285±35	1511-1601 AD (61%) 1616-1664 AD (37%)	1511-1664 AD
GE 283-289	charcoal	220±30	1642-1683 AD (39%) 1735-1805 AD(48%)	1642-1805 AD
GE 103-107	seed	175±30	1657-1696 AD (19%) 1725-1814 AD (55%) 1917-1952* AD (20%)	1657-1952*AD
GE 122-127	seed	170±30	1660-1698 AD (18%) 1722-1817 AD (54%) 1916-1953* AD (20%)	1660-1953* AD
GE 138-142	seed	150±30	1667-1708 AD (17%) 1718-1783 AD (33%) 1796-1827 AD (12%) 1831-1889 AD (19%) 1910-1953* AD (19%)	1667-1953* AD
GE 157-161	seed	205±30	1646-1685 AD (29%) 1732-1808 AD (55%) 1928-1952* AD (16%)	1646-1952* AD
GE 188-193	seed	95±30	1683-1735 AD (28%) 1805-1930 AD (71%)	1683-1930 AD
GE 207-212	seed	125±30	1677-1766 AD (35%) 1800-1895 AD (47%) 1903-1940 AD (16%)	1677-1940 AD
GE 233-238	seed	195±30	1648-1691 AD (25%) 1729-1811 AD (57%) 1922-1952* AD (20%)	1648-1952*AD

860